

# Surface Studies of Pristine and Surface-Modified Polypyrrole Films

X. ZHANG,<sup>1</sup> E. T. KANG,<sup>1,\*</sup> K. G. NEOH,<sup>1</sup> K. L. TAN,<sup>2</sup> D. Y. KIM,<sup>3</sup> and C. Y. KIM<sup>3</sup>

<sup>1</sup>Department of Chemical Engineering, and <sup>2</sup>Department of Physics, National University of Singapore, Kent Ridge, Singapore 0511; <sup>3</sup>Polymer Materials Laboratory, Korea Institute of Science and Technology, P.O. Box 131, Chongryang, Seoul, Korea 130-650

## SYNOPSIS

Polypyrrole (PPY) films having high conductivity were synthesized electrochemically in acetonitrile at low temperature and low current density. Pristine, deprotonated, and ozone-pretreated PPY films were subjected to either thermally induced or near-UV-light-induced graft copolymerization with acrylic acid (AAc), or sodium salt of 4-styrenesulfonic acid (NaSS). Surface structures and redox states of the pristine, deprotonated, reprotonated, and surface-modified polypyrrole films were studied by angle-dependent X-ray photoelectron spectroscopy (XPS). The morphology of the PPY surface after modification by graft copolymerization was revealed by atomic force microscopy (AFM). The results showed that the density of surface grafting decreased with ozone pretreatment. Surface grafting of the two polymeric acids also gave rise to a self-protonated surface structure. A substantial proportion of the grafted protonic acid groups at the surface remained free for further surface functionalization. The surface characteristics, in particular the charge-transfer interactions and the changes in the intrinsic redox states of the substrate films, associated with the external protonation and surface self-protonation processes were also discussed.

© 1996 John Wiley & Sons, Inc.

## INTRODUCTION

In recent years, the synthesis and characterization of electroactive polymers have become an important research area in polymer science.<sup>1</sup> Among these polymers, polypyrrole (PPY) and its derivatives have received a good deal of attention because of their high electrical conductivity, environmental stability, interesting redox properties associated with the chain nitrogens, and ease of synthesis by electrochemical or chemical polymerization.<sup>2-5</sup> Electrochemical polymerization and oxidation offer a relatively simple route for obtaining highly conductive PPY films. In this study, fairly strong and flexible films of polypyrrole doped with *p*-toluenesulfonic acid have been prepared in an electrolyte containing 1% v/v water in acetonitrile.

The fact that the electrical properties of PPY can be drastically modified by various anions,<sup>2,6-8</sup> as well as upon treatment with a strong base or acid<sup>9,10</sup> suggests that PPY and its complexes could be used as active sensing materials in chemical sensors.<sup>11,12</sup> The response behavior of these sensors would be expected to be closely related to the chemical states of the pyrrolylium nitrogens, the nature of the "doping" anions, as well as the interactions between the doping anions and the pyrrolylium nitrogens. Applications of electroactive polymers as active materials for electrodes and sensors will require substantial surface characterization and modification. Surface modifications of conventional polymeric materials to improve biocompatibility for biochemical and biomedical applications have been well reported.<sup>13,14</sup> It has also been demonstrated that surface modifications can be performed through graft copolymerization under mild conditions for a number of polymers, such as polyethylene, poly(ethylene terephthalate), poly(vinylchloride), nylons, and polypropylene, when their surfaces are pretreated

\* To whom correspondence should be addressed.

with high-energy radiation, glow discharge, corona discharge, ozone exposure, or UV irradiation.<sup>15-18</sup> Furthermore, protein and enzyme immobilizations on the surface-modified polymer substrates have also been of great interest.<sup>19</sup>

This study involves a preliminary investigation of surface modifications of PPY films by graft copolymerization with acrylic acid (AAc), and the sodium salt of 4-styrenesulfonic acid (NaSS). Surface grafting of these water-soluble polymers will hopefully improve the hydrophilicity of the PPY film surface and provide appropriate functional groups<sup>19</sup> at the surface for the subsequent immobilization of proteins and enzymes.

X-ray photoelectron spectroscopy (XPS) has been found to be a useful tool for studying polymer-dopant charge-transfer (CT) interactions because of its ability to elucidate the structural changes and the charge redistribution in the complexes associated with these interactions.<sup>9,20-27</sup> It has also provided a convenient means for the quantitative differentiation of the various anion species present in the polymeric complexes. Furthermore, XPS studies on pristine and deprotonated PPY films have demonstrated that the iminelike structure ( $=N-$  structure), aminelike structure ( $-NH-$  structure) and positively charged nitrogens ( $N^+$  structure) corresponding to any particular intrinsic redox state and protonation level of PPY can be quantitatively differentiated in the properly curve-fitted N1s core-level spectrum. They correspond to peak components with binding energies (BEs) at about 397.9, 399.7, and  $> 400$  eV, respectively.<sup>26,27</sup>

## EXPERIMENTAL

### Electrochemical Synthesis of Polypyrrole

Pyrrole monomer was purified by vacuum distillation before use. Acetonitrile and *p*-toluenesulfonic acid were obtained from Aldrich Chem. Co. and nano-pure water was used as an additive solvent. The electrolyte solution of 0.1M *p*-toluenesulfonic acid in acetonitrile containing 1% v/v water was purged for 20 min. with dry nitrogen prior to the addition of the monomer (0.1M pyrrole). Electrochemical oxidation was carried out in a one-compartment cell with a stainless-steel working electrode. The films were grown with a charge density of 10 Coulomb  $cm^{-2}$  at 0°C under dry nitrogen atmosphere and had thicknesses in the range of 5–8  $\mu m$ . The films so prepared has an electrical conductivity of about 200 S  $cm^{-1}$ , as measured by the four-probe technique.

### Deprotonation and Reprotonation of Polypyrrole Films

Some of the as-prepared salt films were deprotonated by treatment with 0.5M NaOH for 16–18 h. After deprotonation, the deprotonated PPY (DP-PPY) films were washed with copious amounts of deionized water. The films were subsequently dried by pumping under reduced pressure. The DP-PPY films were treated with various protonic acids to give rise to reprotonated PPY/anion complexes. The protonic acids used included 1M HCl, 3M HClO<sub>4</sub>, 10% v/v polystyrenesulfonic acid (PSSA), and 0.1M dodecylbenzenesulfonic acid (DBSA). After the treatment the excess acid was removed by pressing the films between two pieces of filter paper. In all cases, the polymer samples were dried by pumping under reduced pressure.

### Surface Modifications

The surfaces of the pristine PPY and DP-PPY films were modified by subjecting them to the following processes: (1) ozone exposure and (2) thermally induced or near-UV-light induced graft copolymerization with acrylic acid (AAc), or the sodium salt of 4-styrenesulfonic acid (NaSS). In all cases, PPY film strips of about 1.5 cm  $\times$  3.5 cm were used. All the pretreated PPY films were subjected to grafting experiments within the same day of ozone treatment. Ozone was generated with an ozone generator (Fischer, Model 500) at an oxygen inlet flow rate of 100 L  $h^{-1}$  and a voltage of 100 V. The ozone production rate was about 3 g  $h^{-1}$ . The mixture of ozone and oxygen was then introduced into a U-shaped glass cell containing the polymer film. The exposure time was varied from about 10 s to 5 min. In the case of surface graft copolymerization, the PPY films, either with or without ozone pretreatment, was immersed in an aqueous solution of 10 wt % AAc or 10 wt % NaSS in a Pyrex tube which was transparent to near-UV light with wavelength  $> 300$  nm. The test tube was purged with nitrogen and sealed off with a silicone rubber stopper. The reaction mixture was then exposed to near-UV light at room temperature ( $\sim 25$ – $28^\circ C$ ) for 40 min. The light source was a 150 W Xe Arc lamp (Kratos Model LH 151). For thermal grafting, the glass tube containing the reaction mixture was placed in a 65°C water bath for 40 min. After each grafting experiment, the PPY film was removed from the viscous homopolymer solution and washed with a jet of deionized water. It was then immersed in a gently stirred,

room-temperature water bath for at least 48 h to remove the residual homopolymer.

### Materials Characterization

XPS measurements were made on a VG ESCALAB MKII spectrometer with a  $MgK_{\alpha}$  X-ray source (1253.6 eV photons). The energy analyzer was set at a constant retardation ratio of 40. The polymer samples in film form were pasted on the standard VG sample studs by means of double-sided adhesive tapes. The core-level spectra were obtained at take-off angles  $20^{\circ}$  and  $75^{\circ}$  (with respect to the film surface). Using 2.5 nm as an effective mean free path for C1s photoelectrons produced by the present X-ray in an organic matrix, the angles correspond to effective depths of about 2 nm and 5 nm, respectively. The pressure in the analysis chamber was maintained at  $10^{-8}$  mbar or lower during the measurements. To compensate for surface charging effects, the binding energies were referenced to the C1s neutral carbon peak at 284.6 eV. In spectral deconvolution, the widths (full width at half-maximum or FWHM) of Gaussian peaks were maintained constant for all components in a particular spectrum. Surface elemental stoichiometries were obtained from peak-area ratios, corrected with the experimentally calibrated sensitivity factors, and might be liable to a maximum of  $\pm 10\%$  error.

For atomic force microscopic (AFM) measurements, a Nanoscope II scanning force microscope was used. Experiments using the repulsive force mode of operation, where the cantilever tip was in permanent contact with the sample surface, were carried out in air. The cantilevers used were supplied by the microscope manufacturer, and had a nominal force constant of  $0.06 \text{ N m}^{-1}$ . The forces applied with the tip were  $\leq 10^{-9} \text{ N}$ . The imaging force was adjusted to just above the pull-off point of cantilever as soon as possible after the first contact in order to reduce the applied force to the minimum possible for stable imaging.

## RESULTS AND DISCUSSION

### Surface of PPY and DP-PPY Film

Previous studies of chemically synthesized PPY have demonstrated that the N1s XPS core-level spectrum of oxidized PPY complexes shows, in general, a major component at a binding energy (BE) of about 399.7 eV, attributable to the neutral pyrrolylium nitrogen ( $-\text{NH}-$  structure) and a high

BE tail above 400 eV, attributable to the positively charged pyrrolylium nitrogen ( $-\text{N}^+\text{H}-$  structure).<sup>20-27</sup> For complexes prepared in a less oxidative environment<sup>22,25</sup> or for complexes "compensated" with a base,<sup>9</sup> a low BE shoulder which is shifted by about  $-2 \text{ eV}$  from the neutral pyrrolylium nitrogen peak is also discernible. This low BE component has been associated with the formation of an imine-like structure ( $=\text{N}-$  structure), as a result of dehydrogenation of a certain fraction of the pyrrolylium nitrogens. Our studies<sup>26-28</sup> on the chemically synthesized PPY have suggested that, as in the case of nitrogens of polyaniline, proton modification of pyrrolylium nitrogens can give rise to a number of intrinsic oxidation states, ranging from that consisting of about 50% iminelike ( $=\text{N}-$ ) structure, through that consisting of 25% imine-like structure (DP-PPY), to that of the fully reduced state consisting of all aminelike ( $-\text{NH}-$ ) structure (PPY<sup>0</sup>). The interconversions between the various intrinsic redox states of PPY are depicted in Figure 1.

Figures 2(a), (b), and (c) show respectively the C1s, N1s, and S2p core-level spectra, obtained at a take-off angle  $75^{\circ}$  (with respect to the film surface), for an electrochemically synthesized (as-prepared) PPY-salt film. The C1s core-level spectrum is dominated by a peak component with a BE at about 284.6 eV, arising from the carbon in the pyrrolylium ring. The high BE tail of the C1s spectrum was curve-fitted with two peaks, corresponding to the CO (ether structure or carbon singly bonded to oxygen) and C=O (carbonyl) species at BEs of 286.4 and 287.7 eV, respectively.<sup>27</sup> The presence of these species may have resulted from surface oxidation or charge-transfer complexing with oxygen. Thus, the surfaces of electrochemically synthesized PPY films have been oxidized to some extent. The presence of surface oxidized species, such as the peroxide or hydroxyperoxide specie, nevertheless, is

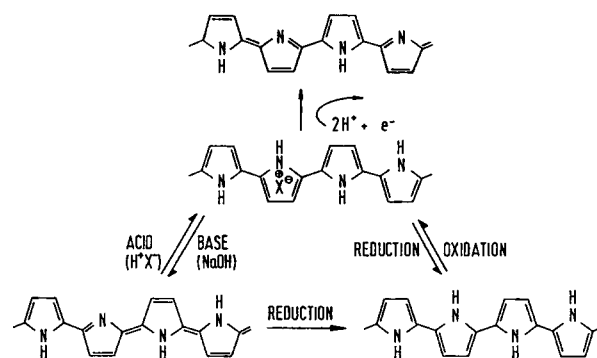


**Figure 1** Interconversion between the various intrinsic redox states in PPY.

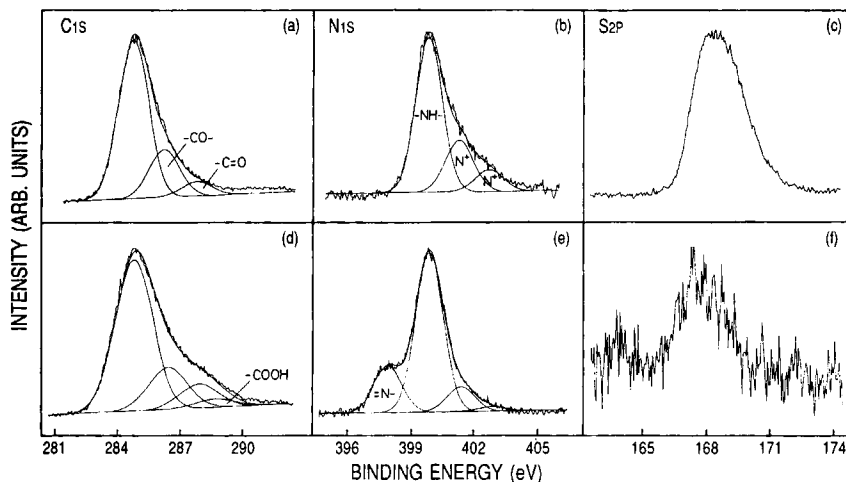


**Figure 2** C1s, N1s, and S2p core-level spectra for (a–c) an as-prepared PPY film, and (d–f) a deprotonated DP-PPY film (XPS take-off angle = 75°).

desirable for the subsequent surface modification via free radical-induced grafting copolymerization. The N1s core-level spectrum has been curve-fitted with components arising from neutral pyrrolylium nitrogen ( $\text{—NH—}$ ) at the BE of  $399.7 \pm 0.1$  eV and positively charged pyrrolylium nitrogen ( $\text{N}^+$ ) at BE above 400 eV. Based on the fixed FWHM approach in peak synthesis, the high BE tail associated with positively charged nitrogens has been resolved into two peaks separated by about 1.4 and 2.8 eV, respectively, from the amine component. The dopant to pyrrole monomer ratio, or the  $[\text{—SO}_3]/[\text{N}]$  ratio, can be readily determined from the sensitivity factors corrected S2p and N1s core-level spectral area ratio (Sample 1, Table I). The fact that the actual protonation level, or the  $[\text{N}^+]/[\text{N}]$  ratio, is lower than the  $[\text{—SO}_3]/[\text{N}]$  ratio suggests that a substantial amount of the dopant exists in the free form. Furthermore, a small proportion of the  $[\text{N}^+]$  com-

ponent may be attributed to the surface oxidized species.

Figures 2(d), (e), and (f) show, respectively, the C1s, N1s, and S2p core-level spectra for the DP-PPY film obtained via the deprotonation of the PPY-salt film in NaOH. Comparison of the XPS C1s core-level lineshape of the as-prepared and the deprotonated PPY films reveals a substantially higher extent of surface oxidation in the DP-PPY film. The increase in the degree of surface oxidation is also indicated by the appearance of a new C1s BE component at about 288.5 eV, attributable to the COOH (carboxylic) species. These results demonstrate that the deprotonation process readily results in the further oxidation of the polymer surface. The appearance of the imine ( $\text{—N=}$ ) component at a BE of 397.9 eV in the N1s core-level spectrum of DP-PPY and the corresponding decrease in the proportion of the  $\text{N}^+$  component and  $[\text{—SO}_3]/[\text{N}]$

**Table I** Surface Structures and Compositions of PPY-Salt Films (Samples 1–4) and DP-PPY Films (Samples 5–8) with Different Ozone Treatment Time (XPS Take-Off Angle = 75°)

Sample No.	O <sub>3</sub> Pretreatment Time (s)	Mole Fraction of				Mole Fraction of			O/N		
		$\text{—CH—}$	$\text{—CO—}$	$\text{—C=O}$	$\text{—COOH}$	$\text{=N—}$	$\text{—NH—}$	$\text{N}^+$	$\text{—SO}_3/\text{N}$	75°	20°
1	0	0.72	0.22	0.06	0	0	0.65	0.35	0.61	1.52	1.65
2	10	0.73	0.18	0.06	0.03	0	0.65	0.35	0.60	2.07	2.36
3	40	0.73	0.15	0.07	0.05	0	0.71	0.29	0.57	2.50	2.56
4	90	0.70	0.15	0.07	0.08	0	0.68	0.32	0.56	2.61	2.56
5	0	0.67	0.18	0.10	0.04	0.20	0.71	0.09	0.03	1.30	1.47
6	10	0.62	0.17	0.17	0.04	0.11	0.80	0.09	0.02	1.33	1.78
7	40	0.51	0.23	0.18	0.08	0.09	0.83	0.08	0.03	1.65	1.94
8	90	0.50	0.22	0.18	0.11	0.09	0.80	0.11	0.02	2.23	2.23

ratio (Sample 5, Table I), are consistent with a deprotonation process. The presence of a residual amount of the  $N^+$  component in DP-PPY may be attributed to the surface oxidized species.

### Surface of Ozone-Treated PPY Films

Figure 3 and Figure 4 provide comparisons for the respective C1s and N1s core-level spectra, obtained at a take-off angle of  $75^\circ$ , of pristine PPY-salt films and the DP-PPY films with different degrees of ozone exposure (0 s, 10 s, 40 s, and 90 s). Treatment of PPY-salt and DP-PPY films with a mixture of oxygen and ozone readily causes a substantial enhancement of the C1s high-BE tail. The surface compositions after various extents of ozone treatment are summarized in Table I. It can be seen that ozone treatment of pristine PPY films causes a decrease of  $-\text{CH}-$ ,  $-\text{CO}-$  species and an increase in the  $-\text{C}=\text{O}$ ,  $-\text{COOH}$  species. This result suggests that the  $-\text{CH}-$  and  $-\text{CO}-$  species were oxidized to the  $-\text{C}=\text{O}$  and  $-\text{COOH}$

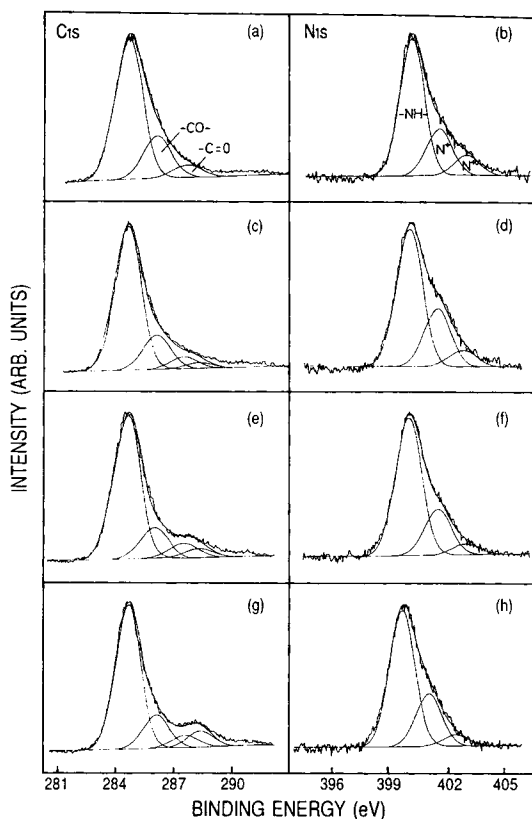


**Figure 3** C1s and N1s core-level spectra for pristine PPY films after (a) and (b) 0 s, (c) and (d) 10 s, (e) and (f) 40 s, and (g) and (h) 90 s of ozone pretreatment (XPS take-off angle =  $75^\circ$ ).

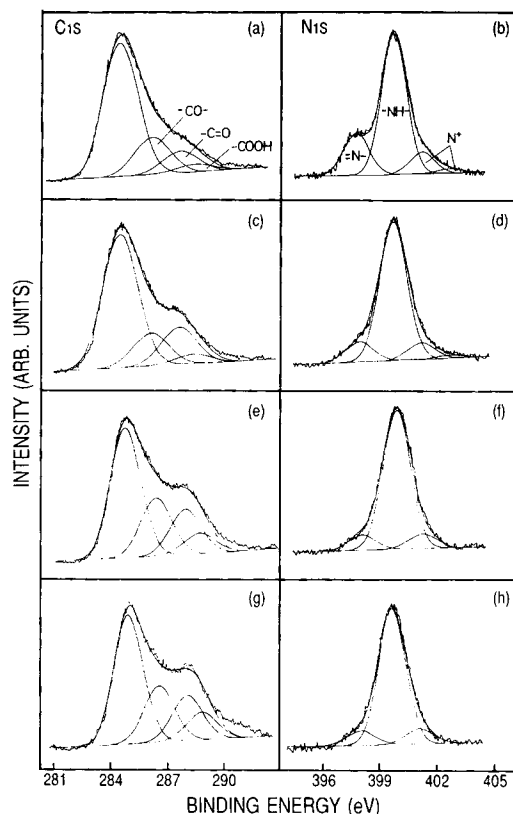


**Figure 4** C1s and N1s core-level spectra for DP-PPY films after (a) and (b) 0 s, (c) and (d) 10 s, (e) and (f) 40 s, and (g) and (h) 90 s of ozone pretreatment (XPS take-off angle =  $75^\circ$ ).

species during ozone treatment. The increase in O/N ratio is consistent with the further oxidation of PPY surface. The oxidation process is also accompanied by a slight decrease in the  $N^+$  species and the release of  $-\text{SO}_3^-$  dopant (Table I). Figure 4 and the data in Table I also show that ozone treatment has a much greater effect on the DP-PPY films, as indicated by the much greater enhancement of the C1s high BE tail. This observation indicates that in the absence of a dopant, DP-PPY is more susceptible to ozone oxidation. The carbon oxidation is also accompanied by a decrease in the intrinsic oxidation state of the polymer associated with the nitrogens. This fact is indicated by the decrease in the concentration of  $=\text{N}-$  species and the increase in the concentration of  $-\text{NH}-$  species (Table I, Samples 5 to 8). Thus, ozone treatment may readily result in extensive oxidative degradation of the PPY film surface, especially in the case of DP-PPY film. Some of the oxidized carbon species in each case is consumed or reduced in the subsequent graft copolymerization process in aqueous medium (see below). In fact, for the present ozone-treated PPY

films, illumination of the film in an aqueous medium with near-UV light readily results in the loss of a substantial amount of the oxidized carbon species. The ease in the reduction of sulfone and sulfoxide species in the ozone-treated thiophene polymers by means of near-UV-light illumination has also been reported.<sup>30</sup>

### Surface of Re protonated PPY Films

The common practice of protonating the polyaniline base powders with volatile acids,<sup>29</sup> HCl in particular, followed by drying under reduced pressure, can result in a substantial removal of the volatile dopant in the surface region. Further removal of the protonic acid readily occurs for complexes exposed to the ultra-high-vacuum environment during surface analyses.<sup>29,32</sup> As a result, the protonation levels or the Cl<sup>-</sup>/N ratios of the HCl protonated polyaniline powder complexes, as revealed by XPS, are usually much lower than 0.5 and protonation is limited mainly to the imine repeating units. As the chemical nature of the nitrogens in polyaniline and PPY is grossly similar, we expect to observe similar results for DP-PPY base during reprotonation.

Figures 5(a) and (b) show the respective N1s and Cl2p core-level spectra obtained at a take-off angle of 75° for a DP-PPY film after protonation by 1M HCl. The corresponding spectra obtained at 20° are shown in Figures 5(c) and (d). The Cl2p core-level spectrum in each case is best resolved into three spin-orbit split doublets [Cl (2p<sub>3/2</sub>) and Cl (2p<sub>1/2</sub>)], with the BE for the Cl (2p<sub>3/2</sub>) peaks lying at about 197.1, 198.6, and 200.2 eV. The first and last BE components suggest the presence of ionic (Cl<sup>-</sup>) and covalent (—Cl) chlorine species, respectively.<sup>33</sup> The intermediate chloride species, Cl\*, which has been widely observed,<sup>34–37</sup> is more appropriately associated with anionic chloride species resulting from the charge transfer interactions between the halogen and the metal-like conducting state of the polymer chain. At both take-off angles, a fairly small imine component exists indicating that HCl is removed during drying under reduced pressure and subsequent exposure to the ultra-high-vacuum environment during surface analysis. The removal of the volatile protonic acid is also consistent with a lower chloride anion/N ratio and a higher —Cl/N ratio observed at the outermost surface of this reprotonated PPY film.

Further depletion of the anionic “dopant” at the surface is achieved upon washing with deionized water. Figures 5(e), (f), (g), and (h) show the corresponding N1s and Cl2p core-level spectra obtained

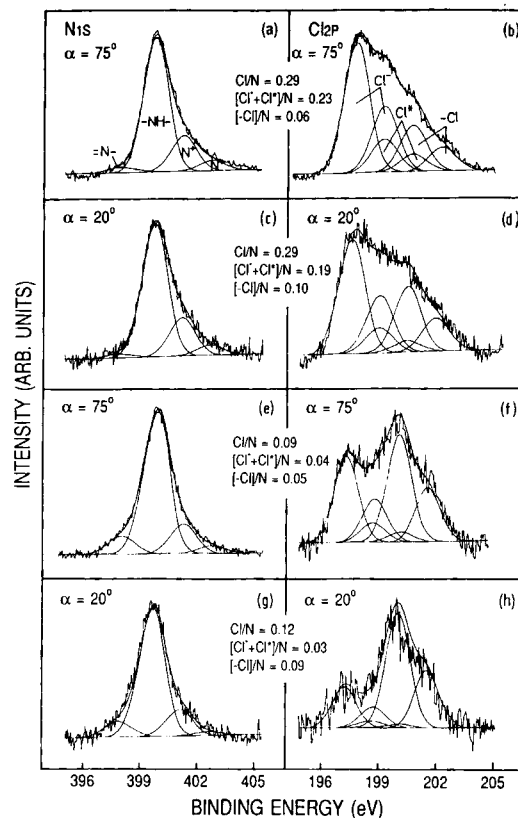


**Figure 5** N1s and Cl2p core-level spectra, obtained at take-off angles ( $\alpha$ 's) of (a) and (b) 75°, and (c) and (d) 20°, of a DP-PPY film reprotonated by 1M HCl. The corresponding spectra at  $\alpha$ 's of 75° and 20° after the film has been washed with deionized water are shown in (e) to (h).

at two take-off angles (75° and 20°) after the film has been washed with deionized water. The removal of the dopant is indicated by a decrease in the anionic Cl/N ratio, the N<sup>+</sup>/N ratio, and the enhancement of the =N— species in the N1s core-level spectra. However, the —Cl/N ratio remains unchanged. The loss of the anionic chloride species is accompanied by the appearance of a corresponding amount of the imine nitrogens. Thus, for the HCl reprotonated PPY film, deprotonation in aqueous medium involves predominantly the lost of HCl.

When the DP-PPY film is exposed to a nonvolatile acid (HClO<sub>4</sub>), the protonation behavior is somewhat different. The anions exist predominantly as the perchlorate species with a characteristic Cl2p<sub>3/2</sub> BE at about 207.5 eV.<sup>27</sup> The respective perchlorate/N ratios for the film, as determined from the corrected Cl2p and N1s core-level spectral area intensity ratios at the two take-off angles of 75° and 20°, are 38% and 43%, respectively and the N<sup>+</sup>/N ratios for the two take-off angles are 27% and 30%, respectively. These results indicate that the proton-

ation level near the top surface is higher than in the bulk for this  $\text{HClO}_4$ -protonated PPY film. This is in sharp contrast to that observed for the DP-PPY film surface protonated by a volatile acid, such as HCl. From the reduction of amine nitrogens (from above 70% normally to below 70%), it is further noted that, in addition to the imine nitrogens, some of the amine nitrogens of the DP-PPY base are also susceptible to protonation.

The protonation of the amine nitrogen in PPY is best observed when the DP-PPY is reprotonated by macromolecular acids. Figures 6(a) and (b) show the N1s core-level spectra, obtained at take-off angles of  $75^\circ$  and  $20^\circ$ , respectively, for a DP-PPY film after being protonated by 10% w/w polystyrene sulfonic acid (PSSA). The differences in the degree of protonation in the surface regions are also discernible from the N1s core-level spectra. The respective  $[-\text{SO}_3]/[\text{N}]$  ratios for the film, as determined from the corrected S2p and N1s core-level spectral area ratios at the two take-off angles, are 1.0 and 1.2. These  $[-\text{SO}_3]/\text{N}$  ratios are consistent with the observation that the proportions of positively charged nitrogens at the two take-off angles, are 85% and 96%, respectively. The fact that the proportions of the amine nitrogens have been reduced to 15% and 4%, in Figures 6(a) and (b), respectively, readily suggests that, in addition to the imine nitrogens, almost all the amine nitrogens of the PPY base are also susceptible to protonation. Protonation levels, or  $[\text{N}^+]/[\text{N}]$  ratios, above 50% can also be readily achieved when DP-PPY base is reprotonated by 0.1M dodecylbenzenesulfonic acid (DBSA). Earlier studies on polyaniline base film protonated by DBSA had also demonstrated a 72% protonation ratio.<sup>38</sup> The high protonation levels observed in the macromolecular acid reprotonated DP-PPY may have resulted from the improved "conformational blending" (at the molecular level) between the PPY chains and the macromolecular dopants. The presence of high protonation level, however, does not result in an increase in the surface conductivity of the film above that of the as-synthesized PPY-TSA film. In fact, the high protonation level may have resulted in the interruption of the polaron-bipolaron lattice.<sup>29</sup>

#### Surface Graft Copolymerization with Acrylic Acid (AAc)

Figures 7(a), (b), and (c) show the respective C1s, N1s and S2p core-level spectra, obtained at a take-off angle of  $75^\circ$ , for a pristine PPY-salt film after being subjected to thermally induced graft copolymerization with AAc. The presence of surface-

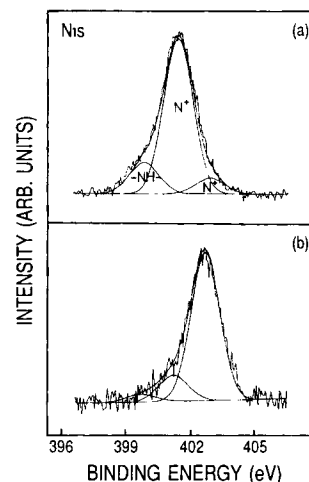


**Figure 6** N1s core-level spectra obtained at take-off angles of (a)  $75^\circ$  and (b)  $20^\circ$ , of a DP-PPY film reprotonated by 10 wt % polystyrenesulfonic acid (PSSA).

grafted AAc polymer is readily suggested by the appearance of a C1s high-BE component at about 288.5 eV, which is associated with the carboxylic acid ( $-\text{COOH}$ ) group of the grafted AAc polymer. Thus the densities of grafting in the surface region can be determined directly from the ratio of the carboxylic acid groups per PPY repeating unit, or the  $[\text{COOH}]/[\text{N}]$  ratio. This ratio can be readily estimated from the sensitivity factors corrected spectral area ratios of the C1s component at 288.5 eV and the N1s core-level spectra. The densities of grafted AAc polymer on the PPY-salt and DP-PPY films as a function of ozone pretreatment time are summarized in Table II based on the core-level signals obtained at a take-off angle of  $75^\circ$ . The density of grafting in each type of film decreases with increasing ozone pretreatment time. This phenomenon is consistent with the overoxidation of the PPY film by ozone as previously mentioned. The fact that graft copolymerization occurs in the PPY films without ozone pretreatment is consistent with the reactive nature of the conjugated polymer surfaces. This reactive nature is apparent from the constant presence of adsorbed or weakly charge-transfer complexed oxygen species on most of the conjugated polymer surfaces. If the core-level signals were obtained closer to the outermost surface, for example at a take-off angle of  $20^\circ$  (Table II, Sample 1b), the density of grafting or the  $[\text{COOH}]/[\text{N}]$  mole ratio for each sample increases substantially compared to the corresponding ratio obtained at a take-off angle of  $75^\circ$ . These results readily indicate that the concentration of the grafted AAc polymer is higher at the outermost surface. In the case of PPY-salt films, almost all the

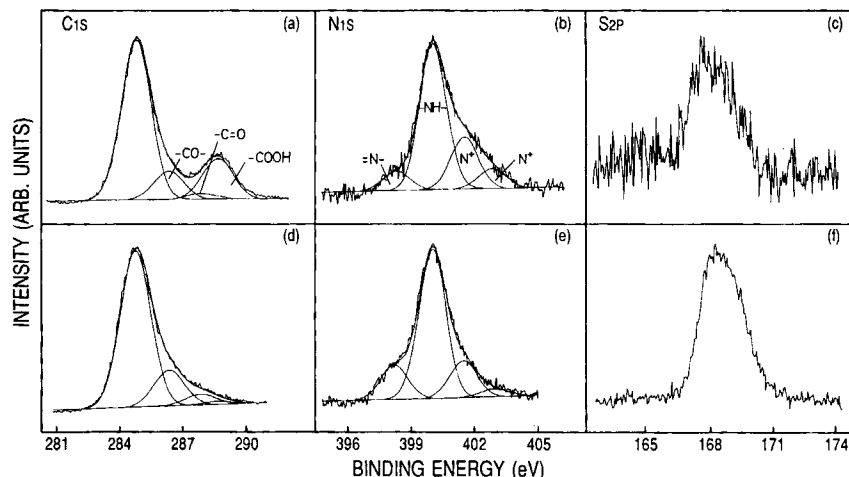


**Figure 7** C1s, N1s, and S2p core-level spectra ( $\alpha = 75^\circ$ ) for (a–c) a pristine PPY-salt film after being subjected to thermally induced graft polymerization in a 10 wt % AAc solution (Sample 1, Table II), and (d–f) a pristine PPY-salt film after being subjected to near-UV-light-induced graft copolymerization in a 10 wt % NaSS solution (Sample 9, Table III).

toluene sulfonic acid dopant in the original films has been removed during graft copolymerization in 10% aqueous AAc solution and the subsequent vigorous washing process after graft copolymerization. This fact is evident from the loss of the S2p core-level signal after grafting of the AAc polymer [Fig. 7(c)]. In fact, prolonged soaking of the electrochemically

prepared PPY-salt film in H<sub>2</sub>O alone can readily result in the deprotonation of the polymer, not unlike that occurs during treatment with a base. The persistence of a large proportion of the N<sup>+</sup> component after graft copolymerization (Table II) thus must have resulted from the protonation of the substrate polymer by the grafted AAc polymer. The ex-

**Table II** Surface Structures and Compositions of PPY-Salt Films and DP-PPY Films after Modification via Graft Copolymerization with Acrylic Acid

Sample No.	O <sub>3</sub> Pretreatment Time (s)	XPS Take-Off Angle (deg)	Graft Density [—COOH]/[N]	Mole Fraction of		
				=N—	—NH—	N <sup>+</sup>
1a	0	75	2.20	0.08	0.62	0.30
1b	0	20	4.00	0.04	0.69	0.27
2	10	75	1.25	0.08	0.70	0.22
3	40	75	1.40	0.07	0.71	0.22
4	300	75	0.83	0.08	0.72	0.20
5a	0	75	0.91	0.08	0.75	0.17
5b	0	20	1.11	0.07	0.76	0.17
6	10	75	0.77	0.08	0.75	0.17
7	40	75	0.62	0.09	0.75	0.16
8	300	75	0.53	0.08	0.74	0.18
9a	0	75	1.60	0.07	0.70	0.23
9b	0	20	2.48	0.04	0.71	0.25
10	10	75	1.57	0.07	0.76	0.17
11	40	75	1.33	0.09	0.76	0.15
12	300	75	1.29	0.08	0.76	0.17

*Note.* Samples 1–4: PPY-salt films after thermally induced graft copolymerization with AAc. Samples 5–8: DP-PPY films after thermally induced graft copolymerization with AAc. Samples 9–12: PPY-salt films after UV-light-induced graft copolymerization with AAc.



istence of a small amount of unprotonated imine nitrogens in this self-protonated surface structure, even in the presence of an excess amount of the COOH groups, suggests that protonation by the surface-grafted polymeric functional groups is less effective and is likely to be governed by the steric effect and molecular conformation of the grafted chains.

Similar surface graft copolymerization behavior is also observed for DP-PPY films (Table II, Samples 5–8) albeit the DP-PPY films are less susceptible to modification via surface graft copolymerization than the pristine PPY-salt films. This is consistent with the more overoxidized surface of the former. Graft copolymerization of DP-PPY film with an AAc polymer readily results in a self-doped or self-protonated surface structure, similar to that observed in the emeraldine base film after graft copolymerization with AAc.<sup>39</sup> The persistence of a small amount of unprotonated imine nitrogens, even in the presence of a large excess of the grafted COOH groups is consistent with the earlier suggestion that protonation by the grafted polymeric functional groups is less effective.

The surface compositions of PPY-salt films after being subjected to near-UV-light-induced graft copolymerization with AAc are also summarized in Table II (Samples 9–12). The grafting densities are similar to those obtained from thermal grafting. Furthermore, a similar effect of ozone pretreatment time on graft density is also observed.

Comparison of the graft densities in Table II with the corresponding  $[N^+]/[N]$  ratios readily suggests that a substantial proportion of the grafted COOH function group remains free at each modified surface. The presence of a large proportion of unreacted carboxylic acid groups on the AAc graft copolymerized PPY surfaces, however, is highly desirable for further surface modification and functionalization. For instance, the carboxylic acid groups can be activated for the immobilization, via chemical bonding, of enzymes and proteins at the PPY surface. This immobilization via a chemical linkage technique is probably more advantageous than the conventional entrapping method.<sup>40</sup> Work on this area is currently in progress.

#### Surface Graft Copolymerization with Na Salt of Styrenesulfonic Acid (NaSS) Polymer

Figures 7(d), (e), and (f) show the respective C1s, N1s, and S2p core-level spectra for a pristine PPY-salt film after it has been modified by near-UV-light-induced surface graft copolymerization with the

NaSS polymer. The presence of the grafted NaSS units is indicated by the S2p core-level spectrum at about 167.8 eV, characteristic of the covalently bonded sulfonic acid group ( $-\text{SO}_3$ ) of the NaSS polymer. In this case, the surface compositions or the densities of surface grafting can be conveniently determined from the sensitivity factor corrected S/N spectral area ratios.

The surface structures and compositions of the PPY and DP-PPY films after surface modification via thermally induced graft copolymerization with NaSS are summarized in Table III (Samples 1–8). Thus, the density of a surface-grafted NaSS polymer decreases with ozone pretreatment in both types of films, and the density of grafting on DP-PPY film is always less than that on the corresponding PPY-salt film. The fact that grafting with a NaSS polymer occurs mainly at the surface region of the PPY film is readily indicated by core-level signals acquired at different take-off angles. For samples measured at a reduced take-off angle of 20° (Samples 1b, 5b, and 9b), a higher density of surface grafting is always observed. Table III also summarizes the surface structures and compositions of the PPY-salt films which were subjected to near-UV-light-induced graft copolymerization with NaSS (Samples 9–12). The dependence of graft densities on ozone pretreatment time and XPS take-off angles are similar to those obtained from thermally induced graft copolymerization. The densities of the surface-grafted NaSS polymer are generally lower than those of surface-grafted AAc polymer under similar experimental conditions.

Although the PPY films after graft copolymerization with NaSS or AAc possess residual imine units (i.e., incomplete protonation of the imine nitrogens due to steric hindrance) and the extent of protonation is not as high as that achievable with external doping by acids, the former is resistant to deprotonation in water. The  $\text{Cl}^-/\text{N}$  ratio of DP-PPY externally doped by HCl decreases from 0.23 to 0.05 after rinsing with deionized water. In contrast, the concentration of  $-\text{SO}_3^-$  groups on PPY surface arising from graft copolymerization with NaSS remain constant even after the films has been soaked for 48 h in deionized water.

#### Surface Morphologies

The changes in the surface morphologies of PPY films after surface modification are shown in the AFM micrographs of Figure 8. The surface of PPY-salt films has a fine granular morphology [Fig. 8(a)]. Deprotonation of the salt film gives

**Table III** Surface Structures and Compositions of the PPY-Salt Films and DP-PPY Films after Modification via Graft Copolymerization with NaSS

Sample No.	O <sub>3</sub> Pretreatment Time (s)	XPS Take-Off Angle (deg)	Grafted Density [—SO <sub>3</sub> ]/[N]	Mole Fraction of		
				=N—	—NH—	N <sup>+</sup>
1a	0	75	0.21	0.15	0.66	0.19
1b	0	20	0.31	0.11	0.69	0.21
2	10	75	0.14	0.11	0.69	0.20
3	40	75	0.13	0.10	0.71	0.18
4	300	75	0.10	0.10	0.76	0.15
5a	0	75	0.10	0.14	0.70	0.17
5b	0	20	0.15	0.10	0.73	0.16
6	10	75	0.09	0.14	0.72	0.14
7	40	75	0.09	0.11	0.72	0.17
8	300	75	0.05	0.15	0.70	0.15
9a	0	75	0.24	0.09	0.68	0.23
9b	0	20	0.33	0.07	0.73	0.20
10	10	75	0.13	0.09	0.73	0.18
11	40	75	0.10	0.09	0.74	0.17
12	300	75	0.09	0.08	0.79	0.13

Note. Samples 1–4: PPY-salt films after thermally induced graft copolymerization with NaSS. Samples 5–8: DP-PPY films after thermally induced graft copolymerization with NaSS. Samples 9–12: PPY-salt films after UV-light-induced graft copolymerization with NaSS.

rise to a base film with coarser granular texture [Fig. 8(b)]. The most drastic change in surface morphologies was observed after modification by graft copolymerization. Figures 8(c) and 8(d) show, respectively, the AFM micrographs of PPY-salt film after graft copolymerization with AAc and that of DP-PPY film after graft copolymerization with NaSS. Thus, the graft copolymerized surfaces all show a striated structure and are less granular in texture. The origin of the striated structure must have resulted from the dehydration of the graft copolymerized surface.

#### Mechanisms of Surface Grafting onto PPY Films

The fact that grafting occurs to some extent in the pristine or untreated PPY films is consistent with the reactive nature of the conjugated polymer surfaces. This is readily supported by the constant presence of adsorbed or weakly charge-transfer complexed oxygen species on most of the conjugated polymer surfaces, as suggested by the presence of a fairly broad and intense O1s spectrum for each sample. The most obvious findings supporting the peroxide mechanism in the present study are the dependence of the density of grafting on the concentration of the surface —CO— species. The latter, in turn, is dependent on the ozone pretreatment

time. When heat or UV light is applied to a PPY film immersed in the monomer solution, radicals are generated on the polymer surface as a result of thermal-induced or photo-induced decomposition of the peroxides. The surface graft copolymerization process is then initiated.

#### CONCLUSION

PPY films synthesized electrochemically are susceptible to surface modification via thermal or near-UV-induced graft copolymerization with AAc and NaSS polymers. In all cases, grafting is limited to the surface region of the PPY film. Thus, XPS has been found to provide a convenient tool for the investigation of the structure and chemical composition at the copolymer interface. The graft density is substantially decreased by ozone pretreatment due to overoxidation of the substrate surface. For external-doping by macromolecular acids, protonation levels above 50% are readily achieved. However, the counterions from external doping are easily removed when exposed to deionized water. On the other hand, the self-protonated surface structure arising from surface graft copolymerization with AAc and NaSS polymers persists even after prolonged exposure in an aqueous medium.

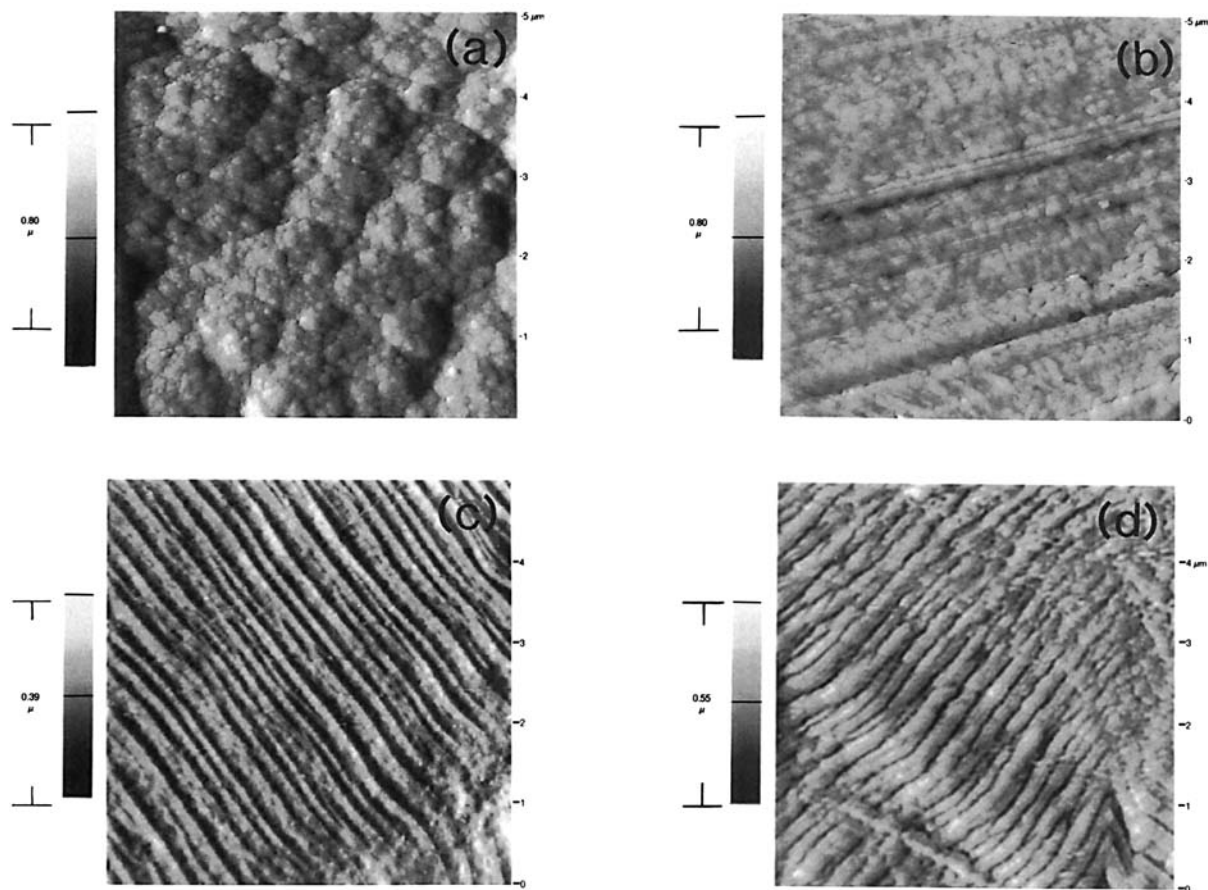


**Figure 8** AFM micrographs of (a) a PPY-salt film, (b) a DP-PPY film, (c) a pristine PPY-salt film after graft copolymerization with AAc, and (d) a 40 s ozone pretreated DP-PPY film after graft copolymerization with NaSS.

## REFERENCES

1. T. Skotheim, Ed., *Handbook of Conducting Polymers, Vols. I and II*, Marcel Dekker, New York, 1986.
2. A. F. Diaz and K. K. Kanazawa, in *Extended Linear Chain Compounds, Vol. 3*, J. S. Miller, Ed., Plenum, New York, 1983, p. 417.
3. G. B. Street, T. C. Clarke, M. Krounbi, K. K. Kanazawa, V. Lee, P. Pfluger, J. C. Scott, and G. Weiser, *Mol. Cryst. Liq. Cryst.*, **83**, 253 (1986).
4. A. Watanabe, M. Tanaka, and J. Tanaka, *Bull. Chem. Soc. Jpn.*, **54**, 253 (1986).
5. V. Bocchi and G. P. Gardini, *J. Chem. Soc. Chem. Commun.*, 148 (1986).
6. J. A. Walker, L. F. Warren, and E. F. Witucki, *J. Polym. Sci. Polym. Chem. Ed.*, **26**, 1285 (1988).
7. T. H. Chao and J. March, *J. Polym. Sci. Polym. Chem. Ed.*, **26**, 743 (1988).
8. E. T. Kang, K. G. Neoh, and K. L. Tan, *Mol. Cryst. Liq. Cryst.*, **173**, 141 (1989).
9. O. Inganäs, R. Erlandsson, C. Nylander, and I. Lundström, *J. Chem. Phys. Solids*, **45**, 427 (1984).
10. G. Gustafsson, I. Lundström, B. Liedberg, G. R. Wu, O. Inganäs, and O. Wennerstrom, *Synth. Met.*, **31**, 163 (1989).
11. T. Hanawa and H. Yoneyama, *Synth. Met.*, **30**, 341 (1989).
12. S. Dong, Z. Sun, and Z. Lu, *J. Chem. Soc. Chem. Commun.*, 993 (1988).
13. J. P. Fischer, U. Becker, S. P. Halasz, K. F. Muck, H. Puschner, S. Rosinger, A. Schmidt, and H. H. Suhr, *J. Polym. Sci. Polym. Symp.*, **66**, 443 (1979).
14. Y. Ikada, in *Advances in Polymer Science 57*, Springer-Verlag: Berlin and Heidelberg, (1984), p. 104.
15. M. Suzuki, A. Kishida, H. Iwata, and Y. Ikada, *Macromolecules*, **19**, 1804 (1986).
16. Y. Uyama and Y. Ikada, *J. Appl. Polym. Sci.*, **36**, 1087 (1988).
17. E. Uchida, Y. Uyama, H. Iwata, and Y. Ikada, *J. Polym. Sci. Polym. Chem.*, **28**, 2837 (1990).
18. Y. Uyama, H. Tadokoro, and Y. Ikada, *Biomaterials*, **12**, 71 (1991).
19. S. Emi, Y. Nurase, T. Hayashi, and A. J. Nakajima, *Appl. Polym. Sci.*, **41**, 2753 (1990).

20. W. R. Salaneck, R. Erlandsson, J. Prejza, I. Lundström, and O. Inganäs, *Synth. Met.*, **5**, 125 (1983).
21. P. Pfluger and G. B. Street, *J. Chem. Phys.*, **80**, 544 (1984).
22. T. A. Skotheim, M. I. Florit, A. Melo, and W. E. O'Grady, *Phys. Rev. B*, **30**, 4846 (1984).
23. R. Erlandsson, O. Inganäs, I. Lundström, and W. R. Salaneck, *Synth. Met.*, **10**, 303 (1985).
24. J. G. Eaves, H. S. Munro, and D. Parker, *Polym. Commun.*, **28**, 38 (1987).
25. M. V. Zeller and S. J. Hahn, *Surf. Interf. Anal.*, **11**, 327 (1988).
26. E. T. Kang, K. G. Neoh, and K. L. Tan, *Surf. Interf. Anal.*, **19**, 33 (1992).
27. E. T. Kang, K. G. Neoh, and K. L. Tan, *Adv. Polym. Sci.*, **106**, 135 (1993).
28. E. T. Kang, K. G. Neoh, Y. K. Ong, K. L. Tan, and B. T. G. Tan, *Synth. Met.*, **139**, 69 (1990).
29. E. T. Kang, K. G. Neoh, Y. L. Woy, K. L. Tan, C. H. A. Huan, and A. T. S. Wee, *Synth. Met.*, **53**, 333 (1993).
30. M. Hanack, G. Hieber, G. Dewald, and H. Ritter, *Synth. Met.*, **41-43**, 507 (1991).
31. A. Ray, G. E. Asturias, D. L. Kershner, A. F. Richter, A. G. MacDiarmid, and A. J. Epstein, *Synth. Met.*, **29**, E141 (1989).
32. E. T. Kang, K. G. Neoh, T. C. Tan, S. H. Khor, and K. L. Tan, *Macromolecules*, **23**, 2918 (1990).
33. G. E. Muilenberg, Ed., *Handbook of X-ray Photoelectron Spectroscopy*, Perkin-Elmer, Minneapolis, KS, 1977, p. 38.
34. K. L. Tan, B. T. G. Tan, E. T. Kang, and K. G. Neoh, *J. Chem. Phys.*, **94**, 5382 (1991).
35. S. R. Mirrezaei, H. S. Munro, and D. Parker, *Synth. Met.*, **26**, 169 (1988).
36. E. T. Kang, K. G. Neoh, Y. K. Ong, K. L. Tan, and B. T. G. Tan, *Macromolecules*, **24**, 2822 (1991).
37. P. Dannetun, R. Lazzaroni, W. R. Salaneck, E. Scherr, Y. Sun, and A. G. MacDiarmid, *Synth. Met.*, **41-43**, 645 (1991).
38. K. G. Neoh, E. T. Kang, and K. L. Tan, *Polymer*, **35**, 2899 (1994).
39. E. T. Kang, K. G. Neoh, K. L. Tan, Y. Uyama, N. Morikawa, and Y. Ikada, *Macromolecules*, **25**, 1959 (1992).
40. M. Umana and Waller, *J. Anal. Chem.*, **58**, 2979 (1986).

Received June 21, 1995

Accepted September 21, 1995